International Journal of Thermodynamics, Vol. 10, No. 2, 1989

Lennard–Jones Fluids in Cavities[1]

A. L. R. Bug[2,3]

Static and dynamic properties of Lennard–Jones particles in spherical cavities of molecular dimension are studied by molecular dynamics (MD) simulation. The local density is a function of the radial coordinate; a layered density profile is reproduced by the iterative solution of an approximate BGY equation. The pair correlation function exhibits a broadened first-neighbor peak and a second-neighbor peak which is shifted inward from its location in the homogeneous fluid. The viscosity, as measured by the relaxation of a rotor in the cavity, is a function of the cavity radius and may actually decrease as the cavity radius decreases. This qualitative trend is reversed when the smooth cavity is replaced by a cavity with rough, molecular walls.

KEY WORDS: dimer; Lennard–Jones; molecular dynamics; porous media; rotational relaxation.

1. INTRODUCTION

The study of fluids which are confined in microscopic pore spaces is of technological and theoretical interest. The behavior of adsorbed molecules within the interiors of micelles [1] or the voids within a microporous structure such as a zeolite [2] is of importance in industrial processes such as catalysis and separation [3]. Further, an adsorbed gas may elucidate the structure of a porous medium, as in the determination of zeolite structure via Xe_{129} NMR [4]. In such a system, the constraints imposed by the walls will play a dominant role in determining structural, thermodynamic, and transport properties of the fluid. Predicting the static and dynamical properties of fluids in micropores is a current theoretical challenge.

[1] Paper presented at the Tenth Symposium on Thermophysical Properties, June 20–23, 1988, Gaithersburg, Maryland, U.S.A.

[2] Department of Chemistry, Columbia University, New York, New York 10027, U.S.A.

[3] Present address: Department of Physics and Astronomy, Swarthmore College, Swarthmore, Pennsylvania 19081, U.S.A.

0195-928X/89/0300-0469$06.00/0

This work treats the structure of a neat fluid of Lennard–Jones (LJ) atoms enclosed in an idealized spherical pore. While a number of recent computer studies have investigated simple fluids (hard sphere and LJ) in sheet and cylindrical pores, only a few have treated fluids in spherical cavities [5–7], and to our knowledge, this is the first molecular dynamics (MD) simulation of such a system.

2. STATIC PROPERTIES

We have simulated a fluid within a constraining pore; briefly, LJ atoms are confined within a spherical region of space of radius R_c. The wall potential is spherically symmetric, and particles within approximately 0.25σ of the wall experience a shallow (<15 K) attractive well terminating in a repulsive potential which varies, to leading order, as $(R_c - r)^{-10}$. The interparticle interaction is considered to be pairwise additive, of LJ 6–12 form, and the strength and range of the interaction are chosen to correspond to xenon: $\varepsilon = 229$ K, $\sigma = 4.05$ Å [8]. The dynamical evolution of the system is simulated by intergrating Newton's equations of motion using a Velocity Verlet [9] algorithm with a time step of the order of 0.0055 ps. For the simulation, the atomic mass was chosen to be 129 proton masses, to correspond to the isotope of xenon, which is a popular NMR probe of zeolitic solids.

Figure 1a shows the density of $N = 10$ and 15 LJ particles as a function of radial position. [Henceforth, unless otherwise noted, all densities are reduced, in units of σ^3. Other reduced quantities are marked with a superscript asterisk and are defined in the conventional way; one LJ time unit is $\sqrt{(m\sigma^2/48\varepsilon)}$.] Cavity radii, R_c, are of the order of 2σ. An average reduced density, ρ^*, is noted, but this quantity is not precisely defined because the free volume in the cavity is not fixed [10]; nor is the uncertainty in volume a negligable boundary contribution. An effective volume may be defined as $4\pi/3\ R_{\text{eff}}^3$, where R_{eff} can be defined from the static density profile as the radial position at which the density falls, say, to 10% of its value. The binding energy of the cavity potential is sufficiently weak so that at the temperatures studied, the enhanced density near the cavity wall is due entirely to the many body correlations between fluid particles. This effect of the exclusion of volume by the particles has been seen repeatedly in previous studies of dense fluids in contact with walls and pore surfaces.

Densities of inhomogeneous fluids have been successfully treated by methods such as mean-field density functional theories [11], density expansions (with various closures) [5, 12], model fluid approaches [13], and an approximate BGY equation [14–16]. The last method has the advantage of being simple to implement for a spherically symmetric wall

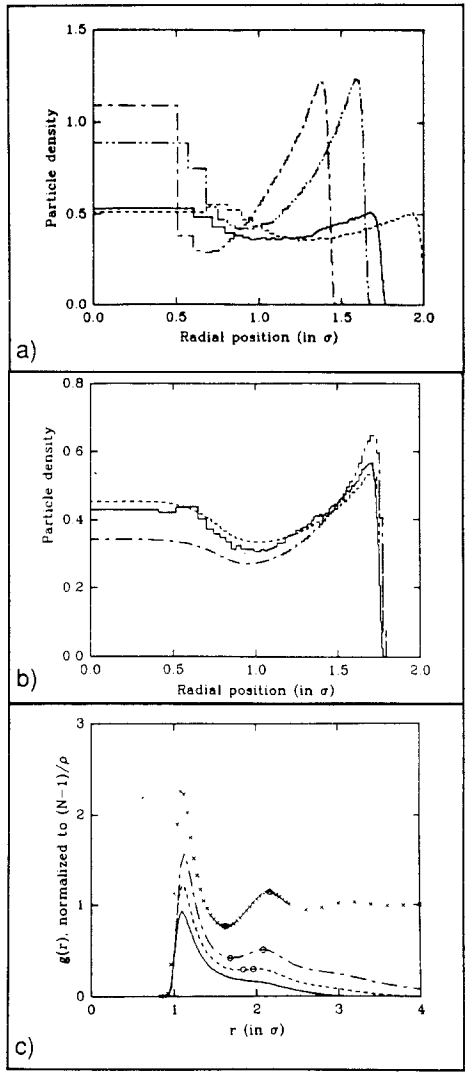

Fig. 1. (a) Reduced density as a function of radial position in cavities of various sizes. $T = 350$ K ($T^* = 1.5$). (——) $N = 10$, $\rho^* = 0.45$; (-----) $N = 15$, $\rho^* = 0.45$; (– – – –) $N = 10$, $\rho^* = 0.8$; (– – – –) $N = 15$, $\rho^* = 0.8$. (b) Inhomogeneous reduced density. $T^* = 3.0$; $N = 10$; $\rho^* = 0.45$. (——) MD simulation; (------) BGY prediction for LJ particles; (– – – –) BGY prediction for hard spheres. (c) $g(r)$, averaged pair correlation function; $T^* = 1.04$, $\rho^* = 0.63$. (——) $N = 10$, $R_c = 1.72\sigma$; (----) $N = 20$, $R_c = 2.12\sigma$; (— — — —) $N = 50$, $R_c = 2.82\sigma$, (×) Data from Ref. 18; (○) extrema of $g(r)$ in second-neighbor region.

potential. To close the heirarchy of integral equations at the level of $\rho(r)$, it employs a hard-sphere approximation for the two-point function, and this has proven successful in recovering the oscillatory profile of dense fluids in contact with solid surfaces. We have used this approach to calculate $\rho(r)$. Details are summarized elsewhere [14, 16, 17]. Briefly, one derives a functional equation for ρ which may be solved iteratively, renormalizing the density after each iteration so that

$$N\sigma^3 = 4\pi \int_0^{R_c} \rho(r)\, r^2\, dr \tag{1}$$

One iterates until $\rho(r)$ has converged to a stable function.

Figure 1b shows an approximate BGY solution along with MD data for the density of a 10-particle system, for $T^* = 3.0$. The agreement is quite close; the approximate solution slightly underestimates (by about 5%) the density near the cavity wall and overestimates the density at the center to a similar extent. For comparison, Fig. 1b also shows the BGY prediction for a cavity filled with hard spheres of the same radius used in the BGY calculation for the LJ particles ($\sigma_{HS} = 0.972\sigma$). This figure suggests that the long-range LJ interaction causes particles to cluster near the center of the cavity, over and above the clustering produced by the packing of hard spheres.

Of physical interest is the likelihood of observing two particles at a given separation. We divide this quantity by ρ^* to obtain an average pair correlation function, $g(r)$, and compare this with the static correlation function of a homogeneous fluid. This is plotted in Fig. 1c, for $N = 10$, 20, and 50; $T^* = 1.04$; and $\rho^* \approx 0.63 \pm 0.05$. Homogeneous data are taken from Verlet [18]. The positions of the first peak for the confined systems are aligned with the first peak in the homogeneous system; the location of the first coordination shell is determined by atomic parameters and not, at these densities, by the wall potential. The amplitude of this peak is greater than that of the first peak in the confined systems, due to the absense of particle density beyond the cavity wall. The neighborhood of the second peak in the homogeneous system changes qualitatively as the system size decreases. As R_c decreases, the positions of the second maximum and minimum (circles) approach each other until they become confluent and vanish, at a cavity radius in the neighborhood of 2σ (between $N = 10$ and $N = 20$).

The shift in the second-neighbor peak of $g(r)$ with R_c indicates an equilibrium fluid structure which is shifted from that of the bulk; this has important consequences for the freezing transition of the confined fluid. However, an altered structure need not be due to the pore geometry; it might owe a great deal to surface and packing effects, which are also responsible for altering the structure of an isolated LJ microcluster.

3. RELAXATION OF A CAGED DIMER

Nonequilibrium MD has been used with success to investigate the shear viscosity of homogeneous fluids [19], but this technique does not generalize readily to an arbitrarily confined fluid. The rotational relaxation of an anisotropic molecule, however, will probe the friction on the molecule (which may then be used to define the "effective" viscosity of the inhomogeneous fluid). In addition, rotational relaxation times are accessible to experiment [20] and often (for example, in the study of an isomerization reaction in a micelle [3]) are of interest because one is directly concerned with the ability of some molecule to reorient in the fluid. For these reasons, we have studied the reorientation of a caged dimer. The dimer consists of two LJ atoms which are rigidly fixed at a given relative separation, d; for this study, $d = 0.8\sigma$. This constraint is achieved with the algorithm "Rattle" [21]. One sees that the dimer atoms are found preferentially in the center of the cavity [29].

To understand the effects of cavity size on the reorientation of the dimer, we plot the expectation value of the first and second Legendre polynomials, $\langle P_i[\mathbf{u}(o)\cdot\mathbf{u}(t)]\rangle$, $i = 1, 2$, in Fig. 2a. The argument of P_i is the cosine of the angle between a unit vector parallel to the dipole axis at some starting time and this vector at later time, t. One averages over starting times and over many (200) realizations of the system. Fluids within cavities of two different radii and a simulated, homogeneous fluid (periodic boundary conditions with the intermolecular potential truncated at 2.5σ) are compared. All three systems share the approximate reduced density $\rho^* = 0.45$. One finds that the relaxation time for the dimer *decreases* as the cavity size decreases. Figure 2b shows the angular velocity autocorrelation function for these systems. The trend in this figure is consistent with the previous result: in the smaller cavity, angular velocity relaxes more slowly and angular position relaxes more quickly; the rotor rotates more freely in the smaller system! In theory, a relaxation time may be defined as the inverse of the integral of a correlation function; however, noise at long times makes this time difficult to obtain accurately. We have chosen two alternative estimates of rotational relaxation times from the data: the first is the slope of a linear region on a log-normal plot of $\langle P_i\rangle$ vs t (if a linear region exists which persists over two or more decades of e) and the second is the time for the correlation function to drop to 0.5. These times are shown in Table I.

The faster orientational/slower dynamical relaxation of the dimer confined in a smaller cavity may seen counterintuitive. As an example of the effect of a spherical boundary on a confined rotor, one may consider the behavior of a spherical rotor of radius r in the center of a cavity of radius

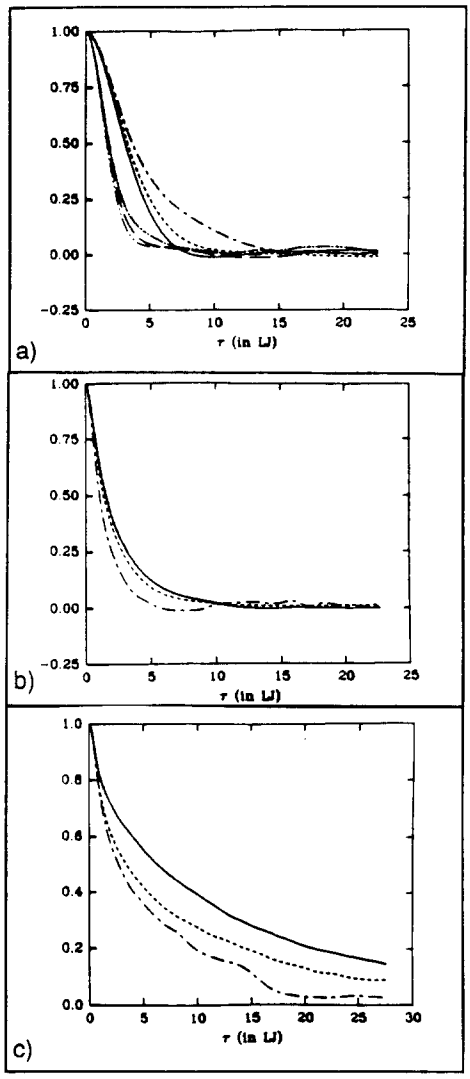

Fig. 2. (a) $\langle P_i[\mathbf{u}(o)\cdot\mathbf{u}(t)]\rangle$. $T=300$ K, $\rho^*=0.45$, $d=0.8\sigma$. (——) $N=10$, $R_c=1.93$, P_1; (-----) $N=15$, $R_c=2.18$, P_1; (------) $N=64$, homogeneous, P_1; (-------) $N=10$, $R_c=1.93$, P_2; (———) $N=15$, $R_c=2.18$, P_2; (–·–·–) $N=64$, homogeneous, P_2. (b) $\langle\omega(0)\cdot\omega(t)\rangle/\langle\omega^2\rangle$ for the systems in a. (c) $\langle P_2[\mathbf{u}(t)\cdot\mathbf{u}(0)]\rangle$ for cavities formed by deleting (——) 38, (-----) 116, and (-----) 260 atom cavities. $\rho^*\approx 0.8$; $T^*\approx 2.5$.

Table I. Relaxation Times for Linear Rotor in Cavity[a]

	$R_c = 1.93$	$R_c = 2.18$	$R_c = \infty$
τ_1^{exp}	—	2.13 ± 0.08	4.14 ± 0.20
$\tau_1^{1/2}$	3.19 ± 0.1	3.36 ± 0.1	3.78 ± 0.1
τ_2^{exp}	0.98 ± 0.08	1.28 ± 0.12	1.58 ± 0.12
$\tau_2^{1/2}$	1.70 ± 0.1	1.81 ± 0.1	1.88 ± 0.1
τ_ω^{exp}	2.6 ± 0.3	2.18 ± 0.11	1.22 ± 0.08
$\tau_\omega^{1/2}$	1.6 ± 0.3	1.4 ± 0.11	1.1 ± 0.08

[a] exp, autocorrelation function fit to exponential at intermediate times; 1/2, time for normalized function to fall to 0.5.

R with a stick hydrodynamic boundary condition. The exact solution for the torque, N, on this sphere is [22]

$$N = -8\pi\eta \frac{r^3 R^3}{R^3 - r^3} \omega \tag{2}$$

where ω is the angular velocity of the sphere. Thus, one may think of the cavity as inducing an effective fluid viscosity of $\eta R^3/(R^3 - r^3)$. If one assumes an exponential model for the relaxation of the angular velocity of the sphere, then the ratio of $\langle N \rangle$ for two systems with identical values of η and temperature and with cavity radii $R_< < R_>$ will be inversely proportionally to the ratio of the two relaxation times. Thus,

$$\frac{\tau_>}{\tau_<} = \frac{R_<^3}{R_>^3} \frac{R_>^3 - r^3}{R_<^3 - r^3} \geqslant 1 \tag{3}$$

Although Eq. (3) applies quantitatively only to exponential relaxation and to spherical rotors, the qualitative trend predicted by hydrodynamics must be that smaller cavities yield a relaxation of angular velocity which is faster than (or equal to) the relaxation in larger cavities with the same bare viscosity η, temperature, and boundary conditions.

It has long been recognized that the molecularity of the solvent may produce rotational friction in a uniform fluid which differs from the predictions of hydrodynamics. For example, theories which consider discrete shells of solvent [23], collisional effects [24], and free spaces in the solution [25] have been proposed. These emphasize the capability of small rotors to engage in "subslip" rotation, in which relaxation behaviors intermediate between hydrodynamic slip and free rotation are observed. The rotation of the caged dimer, since the granularity of the fluid is more pronounced for smaller cavities of the same rough density, may be related

to this phenomenon. The potential of mean force seems to hold the rotor preferentially in the cavity center [29]; an explanation might involve correlated rotation of dimer and solvent shells. Since rotation of the roughly spherical shell of monomers and the walls is a slipping motion, the enhanced rotation of the dimer with its surrounding coordination shell is reminiscent of slip linear flow in a narrow capillary. In a smaller cavity, the smaller amount of ambient solvent simply produces less dissipation of the dimer's rotational motion. Finally, we note that subslip behavior need not be invoked to find the angular relaxation time for the dimer in a uniform fluid. We consider a dense fluid, use $\eta^* = 5.977$ [19] for a fluid with $\rho^* = 1.05$ for $T^* = 2.5$, and substitute into the Perrin [26] expression for the relaxation time for an ellipsoid with an axial ratio corresponding to the dimer (1.8/1). An estimated relaxation time is then $\tau_{\text{stick}} = 62.9LJ$. Hu and Zwanzig [27] have calculated the factor by which one must correct this for a slip hydrodynamic boundary: $\tau_{\text{slip}}/\tau_{\text{stick}} \approx 0.171$, so that $\tau_{\text{slip}} = 10.74LJ$. This is in excellent agreement with a measured value of $\tau = 10.60$ from MD simulation [29]. For the more dilute uniform fluid in Fig. 2a, this value is of the order of $\tau = 3.8LJ$, in reasonable agreement with the data (Table I).

To determine whether the relaxation of the dimer can be attributed to rotational diffusion, one may examine the ratio, τ_1/τ_2, of the relaxation time of $\langle P_1 \rangle$ to that of $\langle P_2 \rangle$. The solution to the angular diffusion equation would predict that $\langle P_i \rangle$ has an exponential form and that the value of this ratio is 3 [28]. From Table I, the ratio of the values of τ bound by modeling $\langle P_i \rangle$ as an exponential gives $\tau_1/\tau_2 = 2.62 \pm 0.35$ and 1.66 ± 0.25 for the homogeneous and 15-particle system, respectively. The former is roughly consistent with diffusion in angle space (although slightly low); the latter is too low. A second condition on angular diffusion is that the relaxation time for angular velocity correlations is much shorter than τ_1. The ratios of these two times are roughly 0.29 and 1.03 for the homogeneous and 15-particle caged system, respectively. Again, the homogeneous system might be reasonably modeled by angular diffusion; the relaxation of the caged dimer has too strong a ballistic character. For these systems, a more general relaxation model, such as extended diffusion [28], seems appropriate; a longer report on these data will appear elsewhere [29].

Our final set of data concerns the dynamics of the dimer in a more realistic molecular pore. An FCC lattice of spherical atoms is constructed, and a cavity is formed by removing successive nearest-neighbor shells of atoms, beginning with a set of six atoms with a cubic symmetry. Around each cavity, two nearest-neighbor layers of solid are allowed to remain, and the rest of the solid atoms are deleted. These atoms form a close packed structure with atomic diameters of unity in LJ units. The cavity is then filled with a dimer and a number of fluid ($d = 0.8$; $\sigma = 1$) atoms which are

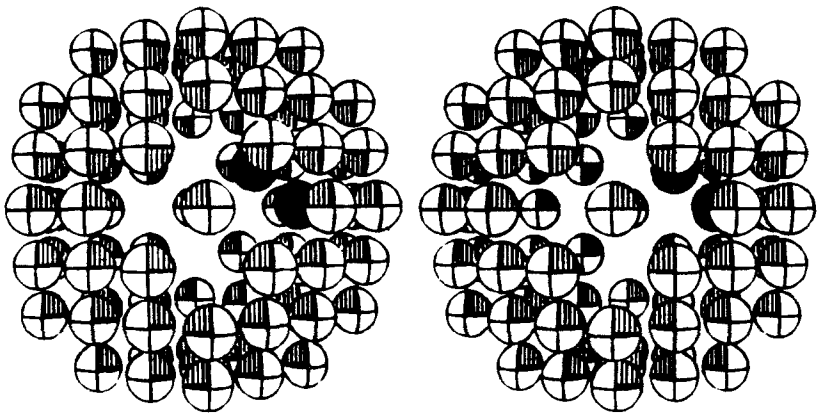

Fig. 3. Stereo view of dimer in 38-atom WCA cavity.

free to move. A stereo view of the dimer in such a cavity is seen in Fig. 3. The fluid–fluid, fluid–dimer potentials are LJ; the potential between the cavity atoms and the fluid atoms is Weeks–Chandler–Anderson [30]. The latter is a LJ potential at short separations which is truncated to a constant value at $r = 2^{1/6}\sigma$, the potential minimum.

Figure 2c shows $\langle P_2[\mathbf{u}(t) \cdot \mathbf{u}(0)] \rangle$ for cavities formed by deleting 38, 116, and 260 close-packed atoms, respectively. [Each of these numbers should be multiplied by $(4\pi/3)/0.74$ to derive the approximate volume of the cavity in units of σ^3.] These cavities were filled with 20, 64, and 145 solvent molecules (plus dimer), respectively, so that $\rho^* \approx 0.8$; $T^* \approx 2.5$. In contrast to the smooth-cavity data, the reorientation of the dimer is significantly slower in the smaller cavities. The relaxation of the dimer in the largest cavity shown is more than a factor of two slower than is the case for the dimer in a homogeneous system at that density.

ACKNOWLEDGMENTS

The author thanks D. F. Coker, G. Martyna, and A. Wallqvist for advice and assistance and is especially grateful for guidance and support from B. J. Berne.

REFERENCES

1. V. Degiorgio and M. Corti (Eds.), *Physics of Amphiphiles: Micelles, Vesicles and Microemulsions* (North-Holland, Amsterdam, 1985).
2. D. W. Breck, *Zeolite Molecular Sieves* (J. Wiley and Sons, New York, 1974).

3. K. Kalyanasundaram, *Photochemistry in Microheterogeneous Systems* (Academic Press, New York, 1987); N. J. Turro, M. B. Zimmt, X. G. Lei, I. R. Gould, K. S. Nitsche, and Y. Cha, *J. Phys. Chem.* **91**:4544 (1987).
4. M. A. Springuel-Huet, T. Ito, and J. P. Fraissard, in *Structure and Reactivity of Modified Zeolites*, P. A. Jacobs et al., eds. (Elsevier, Amsterdam, 1984).
5. E. D. Glandt, *J. Colloid Interface Sci.* **77**:512 (1980).
6. V. V. Nauchitel and A. J. Pertsin, *Mol. Phys.* **40**:1341 (1980).
7. N. Quirke and P. Sheng, *Chem. Phys. Lett.* **110**:64 (1984).
8. J. O. Hirschfelder, C. F. Curtiss, and R. B. Bird, *Molecular Theory of Gases and Liquids* (Wiley, New York, 1954).
9. W. C. Swope, H. C. Andersen, P. H. Berens, and K. R. Wilson, *J. Chem. Phys.* **76**:637 (1982).
10. J. S. Rowlinson, *J. Chem. Soc. Faraday Trans. 2* **82**:1801 (1986).
11. R. Evans, U. M. B. Marconi, and P. Tarazona, *J. Chem. Soc. Faraday Trans. 2* **82**:1763 (1986).
12. D. Henderson, F. F. Abrahan, and J. A. Barker, *Mol. Phys.* **31**:1291 (1976).
13. B. K. Peterson, J. P. R. B. Walton, and K. E. Gubbins, *Int. J. Thermophys.* **6**:585 (1985).
14. J. Fischer and M. Methfessel, *Phys. Rev. A* **22**: 2836 (1980).
15. U. Heinbuch and J. Fischer, *Chem. Phys. Lett.* **135**:587 (1987).
16. T. K. Vanderlick and H. T. Davis, *J. Chem. Phys.* **87**:1791 (1987).
17. A. L. R. Bug and B. J. Berne, Preprint (1988).
18. L. Verlet, *Phys. Rev.* **165**:201 (1968).
19. D. Fincham and D. M. Heyes, *Chem. Phys.* **78**:425 (1983).
20. D. Ben-Amotz and J. M. Drake, Preprint.
21. H. C. Andersen, Preprint.
22. L. D. Landau and E. M. Lifshitz, *Fluid Mechanics* (Pergamon, New York, 1984).
23. A. Gierer and K. Wirtz, *Z. Naturforsch. A* **8**:532 (1953).
24. J. T. Hynes, R. Kapral, and M. Weinberg, *J. Chem. Phys.* **69**:2725 (1978); G. T. Evans, R. G. Cole, and D. K. Hoffman, *J. Chem. Phys.* **77**:3209 (1982).
25. J. L. Dote, D. Kivelson, and R. N. Schwartz, *J. Phys. Chem.* **85**:2169 (1981).
26. F. J. Perrin, *J. Phys. Rad.* **V**:497 (1934).
27. C. Hu and R. Zwanzig, *J. Chem. Phys.* **60**:4354 (1974).
28. B. J. Berne and R. Pecora, *Dynamic Light Scattering* (J. Wiley and Sons, New York, 1976).
29. A. L. R. Bug and B. J. Berne, Preprint (1988).
30. J. D. Weeks, D. Chandler, and H. C. Andersen, *J. Chem. Phys.* **54**:5237 (1971).